Improvement of Wind Power Prediction from Meteorological Characterization with Machine Learning Models

Christiana Sasser[a,b], Meilin Yu[b], Ruben Delgado[c]

[a] *NOAA EPP Earth System Sciences and Remote Sensing Scholar,*
[b] *Department of Mechanical Engineering, University of Maryland, Baltimore County, Baltimore, 21250, MD, USA*
[c] *Joint Center for Earth Systems Technology, University of Maryland, Baltimore County, Baltimore, 21250, MD, USA*

Abstract

To mitigate uncertainties in wind resource assessments and to improve the estimation of energy production of a wind project, this work uses a decision tree machine learning model to assess the effectiveness of hub-height wind speed, rotor-equivalent wind speed, and lapse rate as variables in power prediction. Atmospheric data is used to train regression trees and correlate the power outputs to wind profiles and meteorological characteristics to be able to predict power responses according to physical patterns. The decision tree model was trained for four vertical wind profile classifications to showcase the need for multiple calculations of wind speed at various levels of the rotor layer. Results indicate that when compared to traditional power curve methods, the decision tree combining rotor-equivalent wind speed and lapse rate improves prediction accuracy by 22% for the given data-set, while also proving to be the most effective method in power prediction for all classified vertical wind profile types. Models incorporating lapse rate into predictions performed better than those without it, showing the importance of considering atmospheric criteria in wind power prediction analyses.

Keywords: wind power prediction, machine learning, decision trees, wind energy, vertical wind profiles, rotor equivalent wind speed

1. Introduction

To diminish anthropogenic climate change and curtail global temperature rise, decarbonization of the electricity sector, the largest source of global greenhouse gas emissions, is required. The development of wind energy resources for clean electricity is rapidly growing in the United States, with projections of achieving 20% of wind-derived electricity by 2030, including 202 gigawatts (GW) of onshore wind and 22 GW of offshore wind [1]. As wind power costs have been declining over the past few years, the prevalence of wind energy adoption is growing [2, 3]. Indeed, successful deployment of wind technologies requires accurate prediction of the wind farm power prior to construction and near real-time prediction post-construction for balancing the electricity grid.

During the first stage of developing a wind energy project, the wind and other related factors for a potential project site are measured across the rotor of the turbine and the project area using remote sensing systems and meteorological towers. After the wind resource data has been validated, modeled, and uncertainties have been assessed, the project is then designed and the energy production is estimated [4]. To accurately determine the energy production, predicted losses such as wake effects, turbine availability, electrical losses, turbine performance, environmental effects, curtailment, etc., are taken into consideration when calculating the annual, net energy estimate [4, 5, 6]. Even when these losses and uncertainties are considered, the phenomenon known as the wind farm under-performance bias in which an operational wind farm produces significantly less energy output than the amount expected prior to construction, still exists [7, 8]. A good model estimate of energy production and predicted losses is necessary for accurately determining long-term performance of wind farms.

The Annual Energy Production (AEP) of a wind energy project is determined using the turbine power curve (TPC), which is the power output as a function of kinetic energy flux through the rotor disk of the wind turbine. The power curve equation is as follows,

$$P(t) = \frac{1}{2} c_p \rho A U^3(t) \tag{1}$$

where *P(t)* is the power at a given time t in Watts, c_p is the power coefficient which is the ratio of the power extracted by the turbine to the power of the wind resource (unitless), ρ is the air density in kg/m^3, A is the turbine rotor swept area in m^2, and U is the instantaneous wind speed located at the center of the turbine rotor disk in m/s^2, also known as the hub-height wind speed (HHWS), at a given time t in seconds [9].

The TPC is typically characterized by the cut-in wind speed where the turbine begins to generate power, a sloped region where the power increases at an accelerated rate, the rated speed where the turbine reaches its rated capacity, and the cut-out speed where the turbine shuts down to protect against higher winds [4]. As explained in *Wagner et al.* [10], this method may have been suitable for smaller turbines with lower hub-heights and smaller rotor diameters, but larger turbines are susceptible to varying wind conditions therefore determining the power as a function of hub-height wind speed is not an accurate representation of power.

Although the TPC method may be good for estimations of the power, it cannot be assumed that the turbine produces the expected power at every wind speed and that the HHWS is representative of wind speed throughout the rotor layer. Power output depends on fluctuating wind conditions such as variation in wind speed across the rotor layer and vertical wind variances. Research shows that the vertical wind variance can deviate from the expected power-law shape due to turbines increasing in size, thus increasing exposure to varying wind conditions such as large wind shear and turbulence within the rotor area, which stresses the importance of considering the varying wind speed across the rotor layer [10, 11, 12].

A technique known as Rotor Equivalent Wind Speed (REWS), accounts for varying wind speed throughout the rotor area of a wind turbine by assigning a wind speed to each designated area within the rotor layer of the turbine [13]. In the IEC 61400-12-1 Ed. 2 standard, the use of the REWS term, V_{eq}, (Eq. 2) for estimation of annual energy production for wind turbines is promoted due to its potential in more accurately estimate power production for wind farms [14]. Shown in Figure 1, the rotor area (the circle) is segmented into multiple areas, A_i, and assigned a corresponding wind speed, v_i. This method consists of averaging the weighted wind speed over the rotor sweep area. Note that the figures in this paper have been created by the authors if no specific explanation or reference is given in the caption.

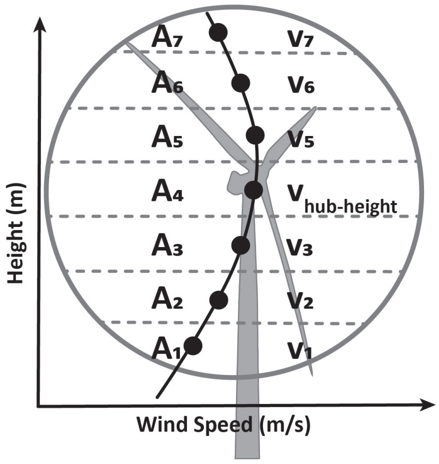

Figure 1: Illustration of Rotor Equivalent Wind Speed, where segments of the rotor area are weighted by associated wind speeds by height.

The equation for the REWS term is as follows,

$$V_{\mathrm{eq}} = \sqrt[3]{\frac{1}{A}\sum_{i=1}^{N} v_i^3 A_i} \tag{2}$$

where V_{eq} is the rotor equivalent wind speed in m/s^2, A_i is the rotor layer area corresponding to the height at the i^{th} rotor layer height in m^2, v_i is the hourly mean wind speed corresponding to the height at the i^{th} rotor layer height in m/s^2, $A{=}\sum_i A_i$ is the entire rotor sweep area in m^2, and N is the total number of measurement heights (unitless).

It has been found that utilizing REWS can better account for variances in vertical wind profiles (VWPs) and can reduce power prediction uncertainty in some scenarios. It was explored in *Wagner et al.* [10] that wind profiles usually do not follow a logarithmic profile; in the case of flat terrain, the shape heavily depends on atmospheric conditions and it was found that measuring the wind speed at multiple points over the rotor sweep area would improve the correlation between wind input and power output. Later, during an experiment where wind speed profiles were measured in front of a multi-megawatt turbine, *Wagner* [15] observed that when REWS was successfully applied, it reduced scatter in the power curve, therefore being less sensitive to shear and less dependent on site which is expected to decrease power curve measurement uncertainty.

However, there have been scenarios where the REWS method provides marginal to no improvement based on atmospheric conditions, turbine design, site location, etc. *Redfern* [16] found that for most situations, use of the REWS has marginal impacts on model forecasts except for scenarios with highly nonlinear wind shear. Similarly, it was found that the usefulness of REWS depends on turbine dimension and wind shear regime, where if the ratio of turbine rotor diameter to hub-height is below 1.8 and the wind shear is constantly between -0.5 and 0.4, the REWS method may not be necessary [17]. During a study within the International Energy Agency Wind Annex 32 designed to test REWS under various conditions, *Wagner* [13] observed that when the power curves for REWS and HHWS were compared, the difference was dependent on the site location. Though more research and analysis are needed to assess what site conditions and turbine designs benefit from the REWS method, this method does demonstrate the susceptibility of the turbine power curve by atmospheric conditions and the usefulness of measuring wind speed across the rotor layer as opposed to at a single instance, such as HHWS.

Power prediction methods, such as the TPC and REWS, only utilizes wind speed as a factor for prediction, without considering the surrounding atmospheric criteria. Studies have shown that variations in atmospheric conditions, such as temperature, atmospheric stability, wind shear, wind direction, and turbulence intensity can be factors in over or underestimation of turbine power output [15, 18, 19, 20, 21]. *Wharton* [22] found that instances with equivalent hub-height wind speeds, but different wind profile shapes would cause a turbine to produce varying power output and that this variability may have been due to atmospheric stability. Since wind is the main function of power, the wind profiles, including factors of wind shear, wind direction, and turbulence, can then be associated with varying atmospheric stability. *Wharton* [22] concluded that power generated under stable conditions was higher than that generated under strongly convective conditions, whereas *Vanderwende* [23] observed that there would be an under-performance in the turbine under stable conditions and an over-performance during convective conditions at moderate wind speeds. Gathering atmospheric criteria other than wind speed may be useful in developing a broader, more accurate picture of the conditions affecting power.

With this shift in analyzing alternate atmospheric criteria, there is also a shift in power estimation techniques towards machine learning models. Machine learning models have been algorithmically improving for wind power forecasting and monitoring [24, 25, 26, 27, 28, 29] but the addition of atmospheric variables into these algorithms has been found to increase the accuracy of predictions [30, 31]. *Clifton* [32] used simulation data of a 1.5-MW turbine to train regression trees to predict the turbine response for combinations of wind speed, wind shear, and turbulence intensity and concluded that the accuracy of the power predictions was three times higher than that from the traditional methodology. In this work, the hub-height wind speed, rotor-equivalent wind speed, and lapse rate, are analyzed as conditions in a machine learning decision tree algorithm. The data has also been classified into four vertical wind profile types to evaluate the relationship between the physical, atmospheric patterns and the turbine power response.

The remainder of the paper is organized as follows: Section 2 gives an overview of the campaign site and available data, gives insight into how the vertical wind profiles and lapse rate were determined, and gives an outline of the machine learning decision tree model implemented in this research. Section 3 presents the results of the decision tree model combinations and the vertical wind profile analysis and discusses further the accuracy of each prediction method and how each method compares to one another. Section 4 gives the conclusions of this research and takeaways.

2. Methodology

2.1. Data Collection

Data used in the analysis of this work was collected in the VERTical Enhanced miXing (VERTEX) field campaign in Lewes, Delaware between September and October of 2016. The purpose of this field campaign was to study the effect of wind turbine wake on the atmosphere-surface exchange of momentum, sensible heat, and water vapor [33]. Many instruments were deployed to collect data on the atmospheric conditions in the field surrounding an operational 2-MW G90 wind turbine with a diameter of 90m and a hub-height of 80m. For the article/study data from a scanning Doppler wind lidar, turbine, and a meteorological (met) tower is used for analysis. Figure 2 shows the location of the Doppler wind lidar, meteorological tower, and turbine. For this research, the lidar and met tower were used to obtain wind measurements and meteorological measurements (such as temperature). The met tower included sensors such as a 3D sonic anemometer and a temperature and relative humidity probe while the scanning lidar included multiple scans explained in detail in *Archer et al.* [33].

Figure 2: A Google Earth [34] visual of the VERTEX Campaign Site and the locations of the scanning Doppler lidar (top), Meteorological (Met) Tower (middle), and 2-MW G90 Wind Turbine (bottom).

To determine the VWP and to not have the lidar measurements influenced by the inflow momentum of the turbine or the wake effect, a Virtual Tower was implemented upstream of the turbine. The Virtual Tower is a column of 10-minute spatially and temporally averaged VWP. To determine the wind speed from the lidar at exact times and a specific location, the Optimal Interpolation (OI) method of lidar retrieval, which is a least-squares method of data assimilation, was implemented [35]. The least-squares method interpolates the available data based on estimated weights that are chosen to minimize error. This method significantly improves velocity retrieval accuracy and preservation of local information compared to other data assimilation methods [36]. The measurements from the OI method that are within the Virtual Tower radius (R) and during the averaged time are divided into their respective height bins, shown in Figure 3, then averaged together according to their bin to create the 10-minute averaged VWPs. The power from the operational wind turbine data was also averaged every 10-minutes to correlate to the wind profiles.

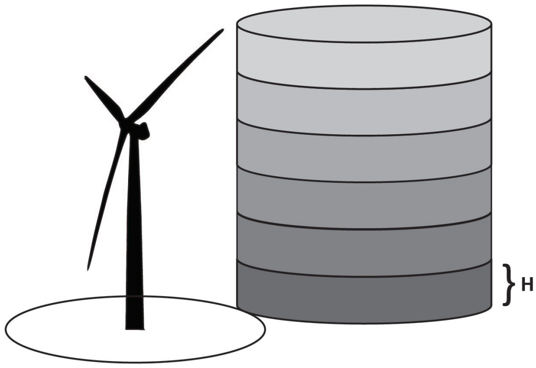

Figure 3: Virtual Tower height bins (cylinder) with respect to the wind turbine. Each height bin is a slice of the Virtual Tower cylinder, denoted by H. Not to scale.

The location of the Virtual Tower, shown in Figure 4, is based on the wind direction, (θ), and a set distance from the turbine, radius (r). The radius around the turbine in the layout is to guarantee that the lidar measurements are not influenced by the movement of the turbine, while the wind direction in the layout was determined by the wind direction captured by the highest point on the met tower (49m).

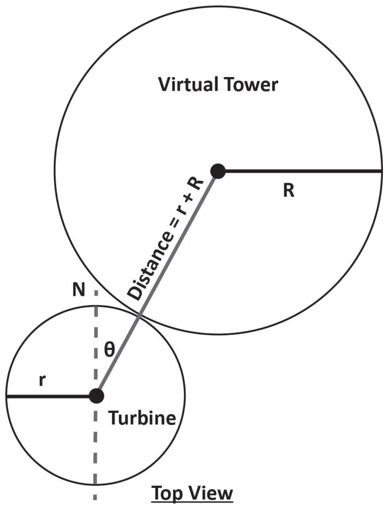

Figure 4: Top view of the Virtual Tower layout with respect to the wind turbine. Virtual Tower (top circle) with radius R and the turbine (small circle) with radius r. The turbine is a distance of (r+R) away from the Virtual Tower. The wind direction is θ a with respect to the North line (dashed line) and the Distance line.

2.2. Lapse Rate

The gradient of temperature results in a gradient in pressure. These differences in air pressure then cause the air to move from the high-pressure area to the low-pressure area, thus causing wind. The larger the difference in temperature and air pressure, the higher the wind speed, and vice versa. This is how temperature affects wind at a basic level. This relationship between temperature and wind speed variances can be applied to differences in temperature with height throughout the atmosphere, affecting vertical wind speed. The lapse rate, the rate of change of temperature with respect to the change in height, was also analyzed in the model. The lapse rate, Γ, is calculated using Eq. 3 as follows,

$$\Gamma = -\frac{dT}{dz}, \tag{3}$$

where T is temperature in °Celsius and z is height in meters [37].

Incorporating an environmental factor that is not wind speed, such as variations of temperature, could give useful insight into the environmental conditions of the site as explained earlier in Section 1. The temperature aspect has the potential to improve power prediction; similarly, to other useful studies which incorporate an atmospheric stability term that uses a temperature parameter [22, 21].

Note that the lapse rate in this study is found using met tower data, therefore, uses five recorded heights of z from 10 m to 49 m. For a more refined analysis of the lapse rate, data from heights within the rotor layer of the turbine should be used.

2.3. Vertical Wind Profile (VWP) Shapes

The VWP shape allows us to better understand the nature of the wind across the lower atmosphere, specifically the rotor layer of the turbine. The VWP shape has the potential to have a significant impact on turbine power estimation; for example, if the wind speed in contact with the turbine blade at the uppermost position in the rotor layer is 10 m/s, while the wind speed in contact with the turbine blade at the lowermost position is 6 m/s, a significant difference in forces would be present on the turbine in that given time.

The VWP is a series of wind speed measurements taken at various heights that show the vertical wind structure in a specific location. VWPs have been shown to deviate from the industry-expected power-law shape, thus, showing the importance of considering wind deviation in the power prediction of wind turbines [11]. The VWP classifications presented in Figure 5 and Table 1 are based on the algorithm used in *St. Pé et al.* [11] and have been implemented into this work. Types 1 and 2, the power law expression and linear expression respectively, are based on the goodness-of-fit criterion for their corresponding mathematical expressions. Types 3 and 4, the relative low-level wind maximum expression and relative low-level wind minimum expression, respectively, are based on relative maximum and minimum wind speed criteria. Note that the tables in this paper have been created by the authors if no specific explanation or reference is given in the title.

Visualization of the four VWP shape classifications is presented in Figure 5. It demonstrates that if a vertical slice of the wind speed from heights z_1 to z_2 were taken across the rotor layer, these are the potential shapes that would be seen. Type 1 is representative of the TPC, as the wind speed does not change much through the rotor layer and can be expressed by the wind speed at the hub-height of the turbine. Type 2 is typical of profiles with wind shear, an increase in wind speed with change in height, thus the linear shape. Types 3 and 4 represent atypical profiles where the wind speed varies significantly from the bottom to the top of the rotor layer.

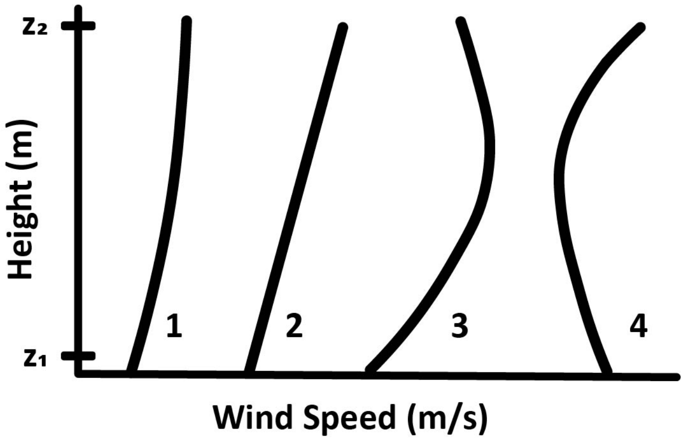

Figure 5: Schematic of the four Vertical Wind Profile shape classifications. Heights z_1 and z_2 indicate the turbine's bottom and top rotor layer measurements.

Table 1: Vertical Wind Profile Classifications.

Types	Expressions
1	Power Law Expression
2	Linear Expression
3	Relative Low-Level Wind Maximum
4	Relative Low-Level Wind Minimum

VWP Type 1 was analyzed using a power law expression and forced fit through the hub-height of the turbine and based on the goodness-of-fit criterion set to the residual sum of squares (RSS) ≤ 0.10. The power law formula is expressed as follows,

$$u(z) = u_{\mathrm{hub}}(\frac{z}{z_{\mathrm{hub}}})^{\alpha} \tag{4}$$

where u_{hub} is the wind speed at hub-height in m/s, z_{hub} is the hub-height in meters, z is the observed height in meters, and α is the power law exponent which is used to analyze the wind shear (unitless) [4, 11].

VWP Type 2 was analyzed using a linear expression and based on the goodness-of-fit criterion set to RSS ≤ 0.10, similarly, to Type 1. The linear fit formula is expressed as follows,

$$f(u) = \beta_0 + \beta_1 u + \epsilon \tag{5}$$

where β_0 is the y-intercept in m/s, β_1 is the slope coefficient (unitless), u is the wind speed at various heights in the profile in m/s, and ϵ is the error term in m/s [11, 38, 39].

VWP Type 3 and 4 were based on the relative maximum and minimum wind speed criteria. The relative maximum formula, Eq. (6), and the relative minimum formula, Eq. (7), are as follows,

$$z_1 < Max\ U_{\mathrm{z}} < z_2 \tag{6}$$

$$z_1 < Min\ U_{\mathrm{z}} < z_2 \tag{7}$$

where $Max\ U_z$ is the height of maximum wind speed in meters, $Min\ U_z$ is the height of minimum wind speed in meters, and z_1 and z_2 are the turbine's bottom and top rotor layer measurements in meters, respectively [11].

Note that in this work, 64% of the data was Type 1, 16% of the data was Type 2, 13% of the data was Type 3, and 7% of the data was Type 4. Having more data points and equal coverage of each VWP could help the model be more refined.

2.4. Machine Learning Overview

With the knowledge of how varying atmospheric criteria and the use of different power estimation techniques affect power prediction of a wind turbine, it is relevant to test the effectiveness of HHWS, REWS, and lapse rate as prediction variables using a machine learning model. Machine learning models are sets of rules that correlate input parameters to output values. The available data is used as both training and testing data. The training data is used to ensure that the model recognizes patterns in the data, while the test data is used to examine how well the machine can predict outputs based on its previous training. The machine learning algorithm creates a model that most effectively maps the inputs of the training data to the associated output values by minimizing the error metric. Then, the error is determined for the testing data to ensure that the model recognizes patterns for all data. This is so the model is not over-fit to the training data, making it too specific and not able to be generalized across data sets. When similar error values for training and testing data occur, a proficient model was created.

We employ regression decision trees, which predict responses to data by following the decisions in the tree from the beginning down to a node, root to leaf [39, 40], to conduct ensemble machine learning of the wind power data. Note that the decision tree is one of the few machine learning models that directly give interpretable outputs from inputs at every decision layer. That is a major reason why regression decision trees are used to perform the current study. The model begins at the root node (i.e., the node on top of the decision tree), which is the first test carried out on the training data-set. From there, based on the outcome, the node branches out to internal nodes that conduct other tests. The tree continues to branch until it reaches the set number of conditions, the maximum number of splits, or desired outcome of the analysis. At the end of the tree, there are leaf nodes, each of which holds a numeric prediction. In the case of this research, the leaf nodes represent the wind power predicted by the regression tree. Note that the mean squared error (MSE) is used as the error metric to calculate the homogeneity of the sample as it branches. The MSE is calculated after every split. The variable with the highest MSE reduction is chosen for the following internal node. The splitting process is continued until a near homogeneous model is created.

An example of a decision tree is shown in Figure 6. The predictor variables used in this example are HHWS and lapse rate while the response variable is turbine power. The model begins at the root node, which is the variable, HHWS with the condition HHWS ≥ 10. The variable and value were chosen for the root node due to having the highest MSE reduction. This node then branches out based on the results of the condition and the MSE calculation. If the HHWS is not greater than or equal to 10 m/s then those results are split to the left internal node HHWS ≥ 5. If the HHWS is greater than or equal to 10 m/s then those results are split to the right internal node HHWS ≥ 15. The internal node, HHWS ≥ 15, then splits to leaf nodes, the resultant response variable, based on the condition. If the HHWS is less than 15 m/s then the result is Power 4. If the HHWS is greater than or equal to 15 m/s then the result is Power 5. On the left side, the internal node, HHWS ≥ 5, splits into another internal node or a leaf node. If the HHWS is not greater than or equal to 5 m/s then the result moves on to the next internal node which uses the predictor lapse rate. The predictor shifted from HHWS to lapse rate due to the MSE reduction being higher using lapse rate at this point in the decision tree. If the HHWS is greater than or equal to 5 m/s then the result is the leaf node, Power 3. The internal node, Lapse Rate ≥ 0.01, is the final test in the decision tree leading to two resultant leaf nodes. If the lapse rate is less than 0.01 then the result is Power 1. If the lapse rate is greater than or equal to 0.1 then the result is Power 2. The result of this decision tree is the data being categorized into Power 1, Power 2, Power 3, Power 4, and Power 5 based on HHWS and lapse rate.

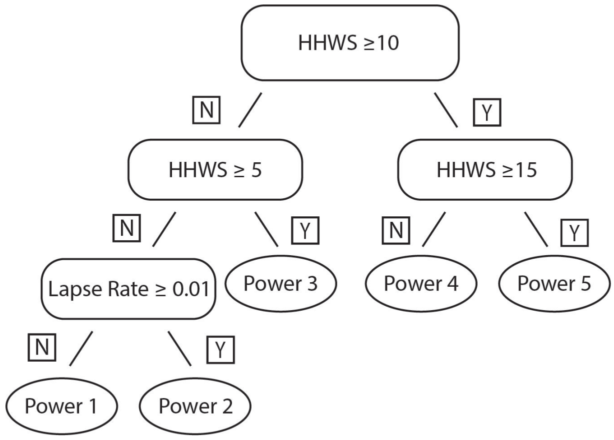

Figure 6: Decision Tree example using two variables, hub-height wind speed and lapse rate, to determine the corresponding powers.

Several regression decision tree models were created to predict power based on different predictors, such as combinations of hub-height and rotor equivalent wind speed, wind profile shape, and lapse rate as shown in Table 2.

Table 2: Decision Tree Predictors.

Decision Tree Labels	**Predictor Variables**
A	HHWS
B	REWS
C	HHWS & Lapse Rate
D	REWS & Lapse Rate

One concern with decision tree methods is that they are prone to over-fitting the data. This means that the data used to train the model is the only data-set the model works well for, and the developed model is not versatile with varying data sets. The k-fold cross-validation was used to add regulation to the optimization problem, thus preventing the over-fit issue [39, 41]. This separates the data into constant k randomly chosen subsets of equal size. In this case, k was chosen to be 5. One subset is used to validate the training model using the remaining subsets. This is then repeated k times so that each subset is used once for the validation process.

Ensemble machine learning methods are used to improve the prediction accuracy of decision trees. This approach can be explained by building a "predictive model by integrating multiple models" [42]. The ensemble methods are implemented in the MATLAB Statistics and Machine Learning Toolbox [39]. The ensemble aggregation method used is Least-Squares Boosting, LSBoost [43]. Note that in this work, the decision trees are not ensembled with different sets of predictors; instead, for a specific predictor combination, the ensemble training is used to boost the prediction accuracy of the corresponding decision tree. This is explained in Algorithm 1 as follows:

In the training ensemble algorithm (Algorithm 1), two functions from MATLAB are being employed: *treeTemplate*, which returns a default decision tree learner template, and *fitrensemble* which uses the LSBoost aggregation to return a training ensemble. For the function *treeTemplate*, the input is the maximum number of splits, *MNS*. The result of this function will be used as a training template in the next function *fitrensemble*. Therein the inputs are the predictor X, the output response variable Y, the number of learning cycles/trees $Number_{Trees}$, the template *Template* built by the function *treeTemplate*, the k-fold cross-validation K_{Fold}, and the learn rate LR. The loop, i, is created to iterate through the number of learn rates: $Number_{LR}$. The LR progresses from 0.1 to 1 in 0.25 increments. Another loop, j, is created to increase tree complexity, which is based on the number of MNS, $Number_{MNS}$. For the *MNS*, the tree-complexity level is exponentially increased for subsequent ensembles from decision stump, one split, to at most n-1 splits, n being the sample size and in the suggested sequence of: 2^0, 2^1... $2^{n\text{-}1}$.

The returned result from the algorithm is the training ensemble, *Model*, which is created from using different combinations of the predictor variables HHWS, REWS, and lapse rate as expressed in Table 2, the response variable, $Number_{Trees}$ (=150) learning cycles/trees, the decision tree learner template, the 5-fold cross-validation, and the learning rates. From this model, the ideal learning rate and ideal maximum number of splits are found and then used to create a final model. All predictions in Section 3 are created using the final model with optimal parameters.

Algorithm 1: Training Ensemble

Input: Input predictor variables: X
Response Variable: Y
Learn rate: LR
Number of Learn Rates: $\mathrm{Number_{LR}}$
Number of maximum number of splits: $\mathrm{Number_{MNS}}$
Maximum number of splits: MNS
Number of learning cycles/trees: $\mathrm{Number_{Trees}}$
Template tree: Template
Number of folds for k-fold: $\mathrm{K_{Fold}}$
Output: Trained regression ensemble model object: Model

for i = *1 to* $Number_{LR}$, **do**
    for j = *1 to* $Number_{MNS}$ **do**
        Template = templateTree(MNS(j))
        Model (j,i) = fitrensemble(X,Y,$\mathrm{Number_{Trees}}$,Template,$\mathrm{K_{Fold}}$,LR(i))
    end
end

3. Results and Discussion

The machine learning model was analyzed using several input predictor variables in varying combinations to test the prediction efficacy of each combination. In this section, how the predictor variables, HHWS, REWS, and lapse rate, affect the power prediction uncertainty will be analyzed. The varying decision tree combinations are shown in Table 2. The data was also divided based on the four VWP Classifications as shown in Table 1, then each decision Tree Combination was analyzed for the given profile.

3.1. Mean Absolute Error

The Mean Absolute Error (MAE), the average difference between each value, was calculated to compare power accuracy and deviations and is expressed as,

$$MAE = \frac{\sum_{i=1}^{n} |(Power_{\text{Predicted}})_i - (Power_{\text{Actual}})_i|}{n} \tag{8}$$

where the $Power_{Predicted}$ represents the power from the decision tree combinations A through D and traditional power prediction methods in kilowatts, the $Power_{Actual}$ in kilowatts is the power output measured from the operational wind turbine in the field experiment, and n is the sample size of the data (unitless).

The MAE calculates the difference between the predicted power and the actual power thus allowing us to compare the various methods, value by value to see how they compare with the operational wind turbine output as shown in Eq. 8. In determining the percent error, the TPC method was used as a basis for comparison since it utilizes the turbine power curve (Eq. 1) and HHWS in its calculation, which is used in the industry. The MAE values can be compared to analyze which method more accurately predicted the power output in comparison to the operational wind turbine and the percent error values can be compared to analyze which method performed well in comparison to the TPC. Lower MAE indicates a better prediction of the turbine response. In this case, the higher the kW value, the more uncertainty, and the lower the kW value, the less uncertainty. In Table 3, the MAE is presented for each prediction method.

Table 3: MAE of Power Prediction Methods

Method	**MAE (kW)**
TPC	182.3
REWS	178.7
Decision Tree A	152.4
Decision Tree B	145.0
Decision Tree C	152.0
Decision Tree D	142.2

In general, the predictions from decision trees are better than those from the traditional methods, such as TPC and REWS. The prediction method that produced the worst MAE was the TPC, which used the power equation and hub-height wind speed. The REWS method gives better prediction due to that it considers the wind profile. Interestingly, when decision trees are used for wind power prediction and analyzed in comparison to the equivalent power curve method, there is significant improvement in the MAE. For example, the decision tree using the equivalent wind speed improves the MAE from the REWS method by 23.2% and the decision tree using the hub-height wind speed improves the MAE from the TPC method by 19.6%. The prediction method that produced the best MAE was the Decision Tree Combination D which was the machine learning model using REWS and the lapse rate as predictors.

3.2. Predicted Power Error Percentages

To convey the positive and negative effects of each variable and power prediction method more vividly, the percent error from the TPC method, shown in Table 4, were calculated using the error equation as follows,

$$Error\ (\%) = \frac{MAE_{\text{Experimental}} - MAE_{\text{TPC}}}{MAE_{\text{TPC}}} \times 100 \tag{9}$$

where the $MAE_{Experimental}$ is the MAE from the decision tree combinations and the REWS method in kilowatts, and the MAE_{TPC} is the MAE from the TPC method in kilowatts. Note that TPC is used as the basis for comparison so that the improvement of the experimental prediction methods upon the traditional power estimation method can be quantified.

Table 4: Power Prediction Error compared to TPC. Note that the "-" sign indicates an error decrease.

Method	Error (%)
REWS	-2.0
Decision Tree A	-16.4
Decision Tree B	-20.4
Decision Tree C	-16.6
Decision Tree D	-22.0

The REWS method improves upon the TPC by 2.0%; though not much, it shows that considering the variability of wind through each area of the rotor layer improves upon the prediction.

To understand how the machine learning decision tree affects the prediction on a fundamental level, the TPC, which uses the HHWS in the power equation (as explained in Section 2),can be compared to the Decision Tree A model that uses the HHWS as the predictor value. This comparison directly shows the differences between using the power equation and the machine learning method. Decision Tree A uses the wind speed at the hub-height of the turbine to predict the power. This model resulted in a 16.4% improvement in power prediction when compared to the TPC. This shows that using a decision tree to predict power using the HHWS rather than a traditional power curve, significantly improves the power prediction.

Tree B, using REWS as a predictor, improves upon the TPC by 20.4%. This is 4% improvement from using HHWS. This is due to the consideration of variable wind speeds throughout the rotor layer, where the wind speed is weighted with the rotor sweep area of the turbine. By considering the variance of wind, the power output can be accurately predicted.

The addition of lapse rate to the first two combinations is also assessed. Tree C, using HHWS and lapse rate as predictors, improves upon the TPC by 16.6%. By pairing lapse rate with HHWS, the model is improved by 0.2% when compared to Tree A, HHWS. Tree D, using REWS and lapse rate as predictors, improves upon the TPC by 22%. By pairing lapse rate with REWS, the model improved 1.6% when compared to Tree B, REWS. Although the improvement seems not significant, as will be presented in the next subsection, substantial wind power prediction improvement shows up when the VWP departures from the power law and linear expressions.

3.3. Machine Learning Predictors Performance by VWP Types

To better assess the performance of decision trees with different predictor combinations, the available data-set was divided into the four VWP Type Classifications and analyzed by each power prediction method. This is to understand if there are methods that work well overall or for specific wind profiles. In Table 5, the performance of decision trees with different predictor combinations, along with each VWP classification type, are presented; their MAEs and the corresponding error percentages in comparison to the TPC are shown. Tree A, with HHWS as the predictor, performs well for the Type 1, Power Law Fits. TPC uses HHWS for its calculations and is assumed to be a power law profile. Therefore, it would make sense for the HHWS predictor to perform well for this wind type. Although this is an improvement in uncertainty reduction, using the wind speed at the hub-height does not consider the potential for differing wind speeds throughout the rotor layer. Tree B, with REWS as the predictor, performs best with respect to the TPC for the Type 3, Low-Level Wind Max Profile. This predictor performs well when the wind profile is non-logarithmic. This is due to REWS accounting for wind speed. Tree C, with HHWS and Lapse Rate as the predictors, and Tree D, with REWS and Lapse Rate as the predictors, both perform well for the Type 3, Low-Level Wind Max Profiles. Profiles classified as Low-Level Wind Max may have temperature profiles that affect wind shape. It is observed that adding lapse rate analysis to the wind speed improves prediction for most wind types.

Table 5: Machine Learning Decision Tree Predictor Combinations with corresponding MAE and error values for each VWP type (Note that the "-" sign indicates an error decrease)

Tree A: HHWS			**Tree B: REWS**		
VWP Type	MAE (kW)	Error (%)	VWP Type	MAE (kW)	Error (%)
1	145.2	-19.9	1	136.9	-24.5
2	149.5	-17.2	2	126.9	-29.8
3	154.5	-19.7	3	129.2	-32.8
4	184.6	14.4	4	151.3	-6.2
Tree C: HHWS, Lapse Rate			**Tree D: REWS, Lapse Rate**		
VWP Type	MAE (kW)	Error (%)	VWP Type	MAE (kW)	Error (%)
1	144.6	-20.2	1	137.2	-24.3
2	151.3	-16.2	2	124.2	-31.1
3	143.2	-25.6	3	125.3	-34.9
4	171.9	6.6	4	145.9	-9.5

As shown in Table 6, the REWS method performed well for Type 3, Low-Level Wind Max Profiles. This is in correspondence with Tree B. Both methods utilizing REWS performed well for this wind type. As seen in Tree B, REWS as a predictor in the decision tree is an improvement upon the TPC for all wind types whereas the REWS method only improves upon the TPC for half of the wind types (Refer to Table 7 for MAE values for TPC in order to compare with the Decision Trees and REWS). Analyzing this progressive method as a predictor in a machine learning model shows promise for analyzing the variability of the wind speed throughout the rotor layer.

Table 6: REWS Method with corresponding MAE and percent error for each VWP type. (Note that the "-" sign indicates an error decrease)

VWP Type	MAE (kW)	Error (%)
1	179.3	-1.0
2	183.1	-1.4
3	158.3	-17.7
4	167.9	4.1

The TPC method performed the best for Type 4, Low-Level Wind Minimum Profiles, as shown in Table 7. The TPC Method is known to overestimate the power based on using a single measure of wind speed at the hub-height of the turbine. This can lead to explaining why this method performed well in some cases and poorly in others. When analyzing a Type 3, Low-Level Wind Maximum profile, the HHWS is the highest wind speed, therefore the power is more overestimated than other types. In the analysis of a Type 4, Low-Level Wind Minimum profile, the HHWS is the lowest wind speed of the profile, therefore the TPC overestimates this low value and, by chance, balances out the wind variance of the profile and is misleading.

Table 7: TPC Method with corresponding MAE for each VWP type.

VWP Type	MAE (kW)
1	181.2
2	180.6
3	192.4
4	161.3

Overall, predictions for Type 4 wind profiles either have marginal improvement or no improvement when compared to the other wind profile classifications. Note that Type 4 accounted for only 7% of the overall data, therefore may not be as accurate as if there was an equal percentage of data for this Type in comparison to the other types. Future research should analyze these wind classifications with a near equal split in data for utmost accuracy.

3.4. Further Discussion

An explanation of the decision tree's superior performance

To further understand why the machine learning decision trees capture the realistic, under-performance of a turbine and the TPC and REWS tend to predict over-performance, the mean power distribution of the methods were examined. In Figure 7, the mean power distribution of the TPC method (first histogram), the REWS method (second histogram), and machine learning decision tree B and D (third and fourth histograms respectively), are shown. There is a slight difference in the TPC and REWS distribution, where in Table 4, the REWS method only improves upon the TPC method by 2%. The machine learning increases the sparsity of the data due to the algorithm clustering the power outputs. Note that even though the TPC and REWS have a more even distribution, these methods also have a large power cluster at around the 2000 kW region, which is the maximum output of the turbine. This explains why these methods calculate an over-performance of the turbine, whereas the decision tree methods capture the under-performance of the turbine, therefore, being more accurate in power prediction.

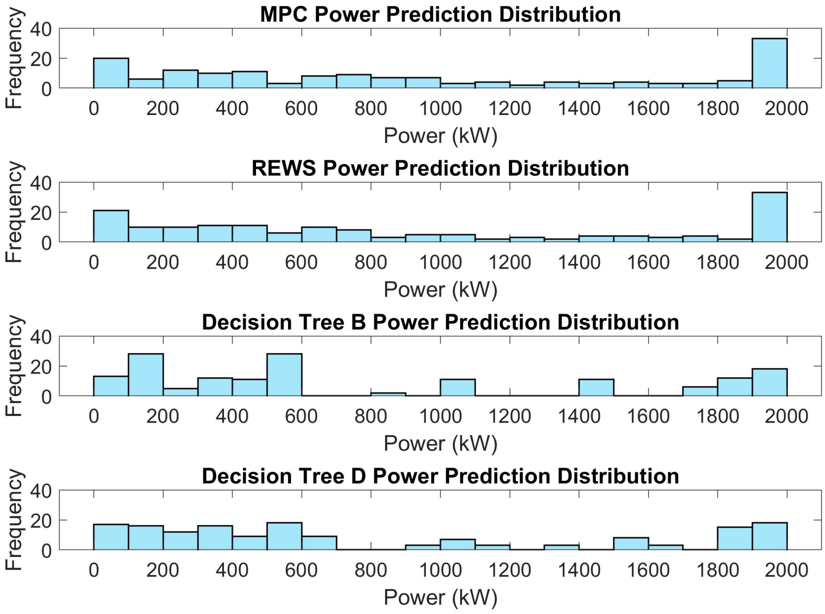

Figure 7: Mean power distribution of TPC method, REWS method, and Decision Tree B and D methods.

Wind shear effect

Note that during this study the wind shear coefficient, α, from the power law expression in Eq. 4 was also tested as a predictor in the decision tree model to represent wind shear. A general overview of the results revealed that using wind shear as a predictor worsened the power prediction of the model. Adding wind shear to HHWS and REWS worsened the prediction by 0.6% and 2.1%, respectively. When analyzed by VWP Type, the addition of wind shear to HHWS improved predictions for Type 2 and 4 as compared to HHWS alone.

However, using wind shear as a predictor does not accurately portray VWP types 3 and 4 because the wind shear coefficients of these profiles are similar and difficult to distinguish from those of Type 1, therefore, the improvement of VWP Type 4 using wind shear may not be an accurate assessment due to the nature of the expressions used to describe the wind profiles. Even with the wind shear coefficient showing marginal improvement for specific profiles, the REWS predictor still outperformed the wind shear and HHWS combination, showing that REWS better considers the wind shear and wind variation in its equation, regardless of wind profile shape. Using the wind shear coefficient from the power law expression is not a good indicator in a decision tree model due to variances in wind profiles.

Lapse rate effect

The lapse rate, determined from the met tower data which was based on five recorded heights ranging from 10 m to 49 m. Though the lapse rate through this height range indicated an improvement in prediction, a calculation of lapse rate throughout the entire rotor layer of the turbine would be useful in refining the model and improving the accuracy of prediction.

4. Conclusion

As wind energy continues to grow, it is vital to utilize various techniques and resources to help mitigate uncertainties in wind resource assessments during pre-construction and to improve the estimation of annual energy production of a wind project to prevent under-performance bias in predictions. In this work, a decision tree machine learning model was implemented to assess the effectiveness of HHWS, REWS, and lapse rate as variables in power prediction. To correlate the power response to physical patterns the model was also assessed for four VWP classifications. Four sets of predictors were used to train and test in the model, HHWS, REWS, HHWS and lapse rate, and REWS and lapse rate. Results demonstrate that using a decision tree model has the potential to better consider the under-performance of a turbine in comparison to traditional power curve prediction methods, while also showing the significance of relating the physical patterns, such as wind profiles, to power outputs to understand the best prediction method for a given pattern. Out of the four predictor sets used, the decision tree model that incorporated REWS and lapse rate had the best overall performance, reducing the predicted power uncertainty by 22% when compared to the TPC method. The combination of REWS and lapse rate into the model also reduced the predicted power uncertainty for all wind profile types tested, especially for those that deviated from a logarithmic-like profile. It was noted that the decision trees that incorporated lapse rate as a predictor performed better than those without lapse rate. This work further demonstrates the utility of machine learning in wind power prediction, the efficacy of measuring wind speeds throughout the rotor layer of a turbine, and the value of finding a relationship between physical patterns and the wind power response.

The keys to moving forward with this method in wind energy power prediction and in wind resources assessments lie in the instrumentation and the training model. The first point is to ensure we have instrumentation installed at the new wind project site with the ability to gather atmospheric data and wind data at various heights for the length of the turbine. The second point is to develop the training model further with more points and turbine powers so that we can generalize the model to alternative locations. If these keys are implemented and prepared for, this method has the possibility of improving wind power predictions from other methods.

Acknowledgements

The authors would like to thank NOAA Educational Partnership Program with Minority Serving Institutions for fellowship support for Christiana Sasser and NOAA Center for Earth System Sciences and Remote Sensing Technologies (Grant number: NA16SEC4810008). The authors also gratefully acknowledge Meredith Sperling from UMBC for helpful discussions and support.

References

[1] P. Gilman, B. Maurer, L. Feinberg, A. Duerr, L. Peterson, W. Musial, P. Beiter, J. Golladay, J. Stromberg, I. Johnson, D. Boren, A. Moore, National Offshore Wind Strategy: Facilitating the Development of the Offshore Wind Industry in the United States, Tech. rep., U.S. Department of Energy and the U.S. Department of the Interior, USA (2016).

[2] A. Duffy, M. Hand, R. Wiser, E. Lantz, A. Dalla Riva, V. Berkhout, M. Stenkvist, D. Weir, R. Lacal-Arántegui, Land-based wind energy cost trends in germany, denmark, ireland, norway, sweden and the united states, Applied Energy 277 (2020) 114777. doi:https://doi.org/10.1016/j.apenergy.2020.114777.
URL `https://www.sciencedirect.com/science/article/pii/S0306261920302890`

[3] E. Williams, E. Hittinger, R. Carvalho, R. Williams, Wind power costs expected to decrease due to technological progress, Energy Policy 106 (2017) 427–435. doi:10.1016/j.enpol.2017.03.032.
URL `https://www.sciencedirect.com/science/article/pii/S0301421517301763`

[4] M. Brower (Ed.), Wind resource assessment: a practical guide to developing a wind project, Wiley, Hoboken, N.J, 2012.

[5] D. Bernadett, M. Brower, S. Van Kempen, W. Wilson, B. Kramak, 2012 BACKCAST STUDY: Verifying AWS Truepower's Energy and Uncertainty Estimates, Tech. rep., AWS Truepower, LLC, Albany, NY (May 2012).
URL `https://aws-dewi.ul.com/assets/2012-Backcast-Study-Verifying-AWS-Truepowers-E`

[6] J. C. Y. Lee, M. J. Fields, An overview of wind energy production prediction bias, losses, and uncertainties, Wind Energy Science Discussions (2020) 1–82doi:https://doi.org/10.5194/wes-2020-85.
URL `https://wes.copernicus.org/preprints/wes-2020-85/`

[7] A. Clifton, A. Smith, M. Fields, Wind Plant Preconstruction Energy Estimates: Current Practice and Opportunities, Technical NREL/TP-5000-64735, National Renewable Energy Laboratory, Golden, CO (Apr. 2016).

[8] C. Johnson, A. Tindal, A. Graves, G. Hassan, Validation of energy predictions by comparison to actual production. (2008).

[9] A. Kalmikov, Wind power fundamentals, in: Wind Energy Engineering, Elsevier, 2017, pp. 17–24. doi:10.1016/B978-0-12-809451-8.00002-3.
URL `https://linkinghub.elsevier.com/retrieve/pii/B9780128094518000023`

[10] R. Wagner, I. Antoniou, S. M. Pedersen, M. S. Courtney, H. E. Jørgensen, The influence of the wind speed profile on wind turbine performance measurements, Wind Energy 12 (4) (2009) 348–362. doi:https://doi.org/10.1002/we.297.
URL `https://onlinelibrary.wiley.com/doi/abs/10.1002/we.297`

[11] A. St. Pé, M. Sperling, J. F. Brodie, R. Delgado, Classifying rotor-layer wind to reduce offshore available power uncertainty, Wind Energy 21 (7) (2018) 461–473. doi:https://doi.org/10.1002/we.2159.
URL `https://onlinelibrary.wiley.com/doi/abs/10.1002/we.2159`

[12] P. Murphy, J. K. Lundquist, P. Fleming, How wind speed shear and directional veer affect the power production of a megawatt-scale operational wind turbine, Wind Energy Science 5 (3) (2020) 1169–1190. doi:https://doi.org/10.5194/wes-5-1169-2020.
URL `https://wes.copernicus.org/articles/5/1169/2020/`

[13] R. Wagner, B. Cañadillas, A. Clifton, S. Feeney, N. Nygaard, M. Poodt, C. S. Martin, E. Tüxen, J. W. Wagenaar, Rotor equivalent wind speed for power curve measurement – comparative exercise for IEA Wind Annex 32, Journal of Physics: Conference Series 524 (2014) 012108. doi:10.1088/1742-6596/524/1/012108.
URL `https://iopscience.iop.org/article/10.1088/1742-6596/524/1/012108`

[14] IEC 61400-12-1:2017, Standard | Wind energy generation systems - Part 12-1: Power performance measurements of electricity producing wind turbines. 2nd Ed., publisher: International Electrotechnical Commission (2017).
URL `https://webstore.iec.ch/publication/26603`

[15] R. Wagner, M. Courtney, J. Gottschall, P. Lindelöw-Marsden, Accounting for the speed shear in wind turbine power performance measurement, Wind Energy 14 (8) (2011) 993–1004. doi:https://doi.org/10.1002/we.509.
URL `https://onlinelibrary.wiley.com/doi/abs/10.1002/we.509`

[16] S. Redfern, J. B. Olson, J. K. Lundquist, C. T. M. Clack, Incorporation of the rotor-equivalent wind speed into the weather research and forecasting model's wind farm parameterization, Monthly Weather Review 147 (3) (2019) 1029–1046. doi:10.1175/MWR-D-18-0194.1.
URL `https://journals.ametsoc.org/view/journals/mwre/147/3/mwr-d-18-0194.1.xml`

[17] W. G. J. H. M. V. Sark, H. C. V. d. Velde, J. P. Coelingh, W. A. A. M. Bierbooms, Do we really need rotor equivalent wind speed?, Wind Energy 22 (6) (2019) 745–763. doi:https://doi.org/10.1002/we.2319.
URL `https://onlinelibrary.wiley.com/doi/abs/10.1002/we.2319`

[18] D. L. Elliott, J. B. Cadogan, Effects of wind shear and turbulence on wind turbine power curves, Tech. Rep. PNL-SA-18354; CONF-900989-2, Pacific Northwest Lab., Richland, WA (USA) (Sep. 1990).
URL `https://www.osti.gov/biblio/6348447`

[19] I. Antoniou, S. M. Pedersen, P. B. Enevoldsen, Wind shear and uncertainties in power curve measurement and wind resources, Wind Engineering 33 (5) (2009) 449–468. doi:10.1260/030952409790291208.
URL `http://journals.sagepub.com/doi/10.1260/030952409790291208`

[20] A. Honrubia, A. Vigueras-Rodríguez, E. G. Lázaro, D. Rodriguez, M. Mejías, I. Lainez, The influence of wind shear in wind turbine power estimation, 2010.

[21] C. M. St. Martin, J. K. Lundquist, A. Clifton, G. S. Poulos, S. J. Schreck, Wind turbine power production and annual energy production depend on atmospheric stability and turbulence, Wind Energy Science 1 (2) (2016) 221–236. doi:https://doi.org/10.5194/wes-1-221-2016.
URL `https://wes.copernicus.org/articles/1/221/2016/`

[22] S. Wharton, J. K. Lundquist, Atmospheric stability affects wind turbine power collection, Environmental Research Letters 7 (1) (2012) 014005. doi:10.1088/1748-9326/7/1/014005.
URL `https://iopscience.iop.org/article/10.1088/1748-9326/7/1/014005`

[23] B. J. Vanderwende, J. K. Lundquist, The modification of wind turbine performance by statistically distinct atmospheric regimes, Environmental Research Letters 7 (3) (2012) 034035. doi:10.1088/1748-9326/7/3/034035.
URL https://iopscience.iop.org/article/10.1088/1748-9326/7/3/034035

[24] H. Acikgoz, C. Yildiz, M. Sekkeli, An extreme learning machine based very short-term wind power forecasting method for complex terrain, Energy Sources, Part A: Recovery, Utilization, and Environmental Effects 42 (22) (2020) 2715–2730. doi:10.1080/15567036.2020.1755390.
URL https://www.tandfonline.com/doi/full/10.1080/15567036.2020.1755390

[25] H. Demolli, A. S. Dokuz, A. Ecemis, M. Gokcek, Wind power forecasting based on daily wind speed data using machine learning algorithms, Energy Conversion and Management 198 (2019) 111823. doi:10.1016/j.enconman.2019.111823.
URL https://www.sciencedirect.com/science/article/pii/S0196890419308052

[26] J. Heinermann, O. Kramer, Machine learning ensembles for wind power prediction, Renewable Energy 89 (2016) 671–679. doi:10.1016/j.renene.2015.11.073.
URL https://www.sciencedirect.com/science/article/pii/S0960148115304894

[27] N. Li, F. He, W. Ma, Wind power prediction based on extreme learning machine with kernel mean p-power error loss, Energies 12 (4) (2019) 673. doi:10.3390/en12040673.
URL https://www.mdpi.com/1996-1073/12/4/673

[28] A. Marvuglia, A. Messineo, Monitoring of wind farms' power curves using machine learning techniques, Applied Energy 98 (2012) 574–583. doi:10.1016/j.apenergy.2012.04.037.
URL https://linkinghub.elsevier.com/retrieve/pii/S0306261912003236

[29] C. Carrillo, A. Obando Montaño, J. Cidrás, E. Díaz-Dorado, Review of power curve modelling for wind turbines, Renewable and Sustainable Energy Reviews 21 (2013) 572–581. doi:https://doi.org/10.1016/j.rser.2013.01.012.
URL https://www.sciencedirect.com/science/article/pii/S1364032113000439

[30] M. Optis, J. Perr-Sauer, The importance of atmospheric turbulence and stability in machine-learning models of wind farm power production, Renewable and Sustainable Energy Reviews 112 (2019) 27–41. doi:10.1016/j.rser.2019.05.031.
URL https://www.sciencedirect.com/science/article/pii/S1364032119303442

[31] J. Nielson, K. Bhaganagar, R. Meka, A. Alaeddini, Using atmospheric inputs for Artificial Neural Networks to improve wind turbine power prediction, Energy 190 (2020) 116273. doi:10.1016/j.energy.2019.116273.
URL https://www.sciencedirect.com/science/article/pii/S0360544219319681

[32] A. Clifton, L. Kilcher, J. K. Lundquist, P. Fleming, Using machine learning to predict wind turbine power output, Environmental Research Letters 8 (2) (2013) 024009. doi:10.1088/1748-9326/8/2/024009.
URL https://doi.org/10.1088/1748-9326/8/2/024009

[33] C. L. Archer, S. Wu, A. Vasel-Be-Hagh, J. F. Brodie, R. Delgado, A. St. Pé, S. Oncley, S. Semmer, The VERTEX field campaign: observations of near-ground effects of wind turbine wakes, Journal of Turbulence 20 (1) (2019) 64–92.

doi:10.1080/14685248.2019.1572161.
URL https://www.tandfonline.com/doi/full/10.1080/14685248.2019.1572161

[34] G. E. P. 7.3.4.8248, Lewes, Delaware, TerraMetrics 2021 (June 2018).
URL http://www.google.com/earth/index.html

[35] A. Choukulkar, R. Calhoun, B. Billings, J. D. Doyle, A modified optimal interpolation technique for vector retrieval for coherent doppler lidar, IEEE Geoscience and Remote Sensing Letters 9 (6) (2012) 1132–1136. doi:10.1109/LGRS.2012.2191762.
URL http://ieeexplore.ieee.org/document/6193408/

[36] S. Kongara, R. Calhoun, A. Choukulkar, M.-O. Boldi, Velocity retrieval for coherent Doppler lidar, International Journal of Remote Sensing 33 (11) (2012) 3596–3613. doi:10.1080/01431161.2011.631948.
URL https://www.tandfonline.com/doi/full/10.1080/01431161.2011.631948

[37] J. M. Wallace, P. V. Hobbs, Atmospheric science: an introductory survey, 2nd Edition, no. v. 92 in International geophysics series, Elsevier Academic Press, Amsterdam ; Boston, 2006, oCLC: ocm62421169.

[38] Linear regression - MATLAB & Simulink (Date Accessed: 2021-02-25).
URL https://www.mathworks.com/help/matlab/data_analysis/linear-regression.html

[39] MATLAB R2018b 9.5.0.944444 (2018).

[40] Decision trees - MATLAB & Simulink (Date Accessed: 2021-02-25).
URL https://www.mathworks.com/help/stats/decision-trees.html

[41] Cross-validation - MATLAB & Simulink (Date Accessed: 2021-02-25).
URL https://www.mathworks.com/discovery/cross-validation.html

[42] L. Rokach, Ensemble-based classifiers, Artificial Intelligence Review 33 (1-2) (2010) 1–39. doi:10.1007/s10462-009-9124-7.
URL http://link.springer.com/10.1007/s10462-009-9124-7

[43] J. H. Friedman, Greedy function approximation: A gradient boosting machine., The Annals of Statistics 29 (5) (2001) 1189–1232. doi:10.1214/aos/1013203451.
URL http://projecteuclid.org/euclid.aos/1013203451